Development of a post-processing pipeline for Myelin Water Imaging at 7 T

Elliot Berthold (BME–19), Petter Clemensson (BME–19)

***Abstract*—Myelin water imaging, MWI, is a non-invasive method used for quantifying the amount of myelin in the brain that can aid the understanding of brain plasticity and neurodegenerative diseases, such as Multiple Sclerosis (MS). Conventional MWI is done at a field strength of 3 T, though there are indications that higher field strength may lead to higher resolution images. We investigate the use of isotropic voxels and echo time (TE) 8 ms at 7 T MWI, establish favorable parameters, and compare our results with a previous study, where anisotropic voxels and TE 10 ms were used. Moreover, we aim to demonstrate the usefulness of MWI at 7 T and further develop it by looking at a pilot data set consisting of diagnosed MS patients and comparing our results to an extensive 3 T MWI atlas. Healthy individuals were scanned using 8 ms and 10 ms TE, along with a pilot dataset consisting of scans from MS patients using 8 ms TE at 7 T. We have demonstrated that MWI on 7 T scans with isotropic voxels and an 8 ms TE can be used to identify lesions associated with MS. Although 8 ms TE performed equally well as the established 10 ms TE when it comes to the characterization of the myelin water fraction, there is not enough evidence to validate that an 8 ms TE is superior to 10 ms. Further research is warranted to evaluate the possibility of generalizing the 3 T MWI atlas across field strengths.**

***Index Terms*—Magnetic Resonance Imaging, Myelin Water Imaging, Neuroimaging,**

I. Introduction

Magnetic Resonance Imaging (MRI) is a non-invasive medical imaging technique used for depicting the anatomy and physical processes in, for example, the brain. Within conventional MRI, the depicted image is assessed by a radiologist to identify pathological differences [1]. The nature of this type of data is typically qualitative, which can make it challenging to study the progression of neurodegenerative diseases. Patients with such a disease routinely do MRI scans, but pathological changes between scans can be small, making it hard to accurately forecast the disease progression [2]. By enabling more advanced statistical analysis, quantifying this information is one step toward better understanding the course of the disease and providing clinicians with an opportunity to develop personalized medicine, thereby increasing patient outcome [3].

A. Myelin Water Imaging

This paper investigates a quantitative MRI method known as myelin water imaging (MWI), which provides an MRI signal specific to myelin (insulating sheaths that form around nerves) that enables visualization of myelination in the brain and spinal cord in vivo [4]. A specific measure of myelin content has important implications for understanding brain plasticity and neurodegenerative diseases, particularly Multiple Sclerosis (MS) [5], [6]. However, quantifying MRI data is challenging as it often involves solving an inverse problem. Briefly, the inverse problem in MWI can be described as a mathematical model involving a decaying, multi-exponential signal and free parameters that remain to be specified. This problem can be simplified with two components that decay exponentially (one slow and one quick), the signal ($S(t)$) can be expressed as

$$S(t) = c_{short} \cdot e^{-t/T_{2,short}} + c_{long} \cdot e^{-t/T_{2,long}},$$

where $T_{2,short}$ and $T_{2,long}$ characterize the relaxation time (T_2 time) of each component with a corresponding population c_{short} and c_{long}. In reality, the general equation that describes multiexponential relaxation–in particular the fundamental MWI-model–is a sum of nT_2 components defined as

$$S(t) = \sum_{n=1}^{nT_2} c_n \cdot e^{-t/T_{2,n}}, \tag{1}$$

where the short and long components consist of multiple subcomponents, n, with their own relaxation time, $T_{2,n}$, and population, c_n. The number of T_2 times (nT_2) used to model MWI is typically around 40 [7]. The sub-components associated with the short and long are defined within a range of relaxation times. As indicated, the short component decays quickly while the long component decays slowly. As discovered in 1994 by MacKay et al., these components reflect different tissue types' water content in the brain [4]. As illustrated in figure 1, water bound between myelin sheaths have a short relaxation time, while water in the cytoplasmic space, extracellular space, and cerebrospinal fluid have a longer relaxation time. At 3 and 7 Tesla MRI, the short component has a relaxation time in the range of $8 - 30$ ms and $8 - 20$ ms, respectively [8]. As exemplified in figure 1-B, one can identify two components, and by defining a cut-off, one can define the myelin water fraction (MWF) as the area under the curve within the interval between a minimum T_2 time ($T_{2,min}$) and a T_2 cut-off time ($T_{2,cut}$) divided by the total area under the curve. Mathematically, MWF can be expressed as

$$MWF = \frac{\sum_{n=min}^{n=cut} c_n}{\sum_{n=min}^{n=max} c_n}.$$

In that sense, the short fraction (purple area in figure 1-B) is an indirect measurement of the fraction of water associated with myelin sheaths. A common way of visualizing this fraction is by plotting the T_2 distribution, as seen in figure 1-B. *In*

Published June 16, 2022
E-mail: elliot.berthold@gmail.com, petter@clemensson.com
Technical supervisor: Emil Ljungberg, Dep. of Medical Radiation Physics
Clinical supervisor: Gunther Helms, Dep. of Medical Radiation Physics

vivo MWI is an established method at 3 T MRI but has been absent at 7 T until recently. Higher field strength allows for a more measurable signal and thus a higher signal-to-noise ratio, which allows for higher resolution [9]. The benefit of the high resolution has been shown to be an important factor in MWI on the spinal cord due to its notably tiny structures [10]. Although the brain has more pronounced structures, it can be a clinical benefit to combine MWI with a higher field strength to highlight minor variations and structures in the brain. A thorough exposition of inverse problems in MRI and a comprehensive description of MWI can be found elsewhere [11]–[13].

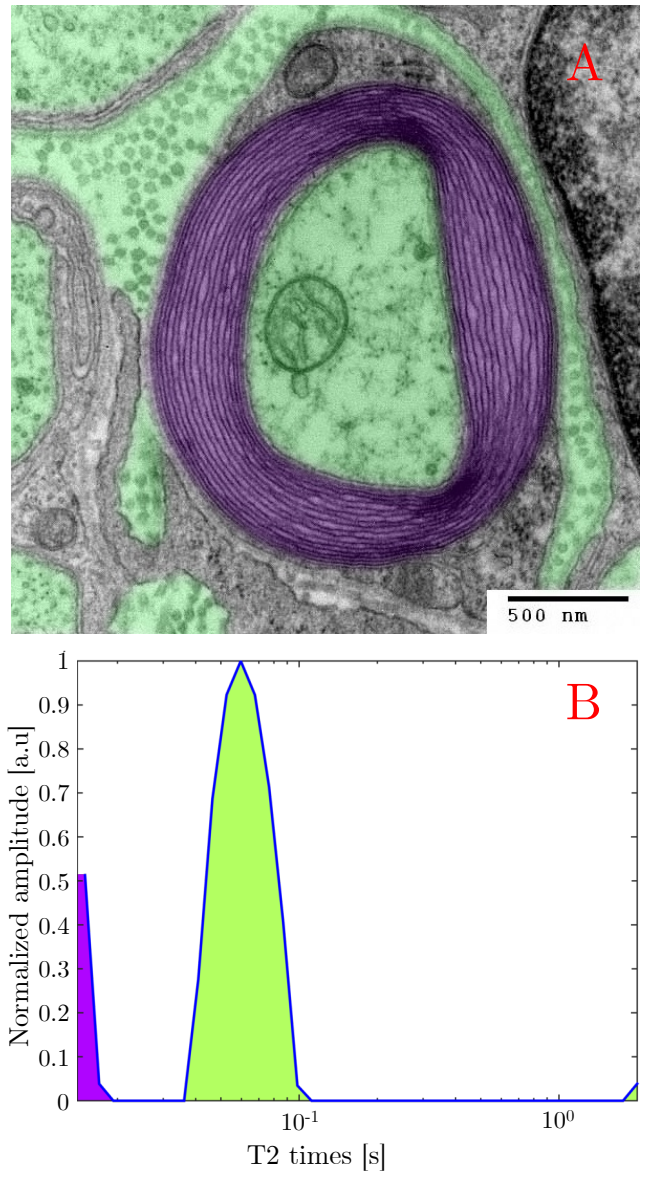

Fig. 1. A shows a cross-section through an axon with the location of cytoplasmic and extracellular water (green) and myelin water (purple). B illustrates an example of a T_2 distribution of human white matter *in vivo*. The short and long components mentioned in connection with equation 1 correspond to the purple and green areas. Note the small hump to the right. It represents water in the cerebrospinal fluid, having a considerably longer relaxation time than the other compartments. Adaptation of [14]. Image courtesy of Emil Ljungberg.

B. Aim of this study

Our project came about because it has not been investigated how to analyze MWI data with an echo time (TE) of 8 ms and isotropic resolution collected at a field strength of 7 Tesla. As of June 16, 2022, one paper has been published regarding *in vivo* MWI at 7 T compared to 3 T [8]. However, with anisotropic voxels and longer TE.

There are many advantages to switching to a different voxel shape and shorter echo time (TE). Regarding voxel shape, switching from rectangular cuboidal to cubical (i.e., anisotropic to isotropic voxels) is beneficial. The advantage of isotropic voxels is that anatomical structures become clearer overall than anisotropic voxels, ultimately expanding studies from one to three planes [15]. Having a shorter TE should improve the characterization of the short T_2 component, which is what corresponds to the myelin water fraction (MWF). Reflecting myelin content in each voxel, the MWF becomes the principal quantity calculated in MWI.

Moreover, we aim to demonstrate the usefulness of MWI at 7 T and further develop it by looking at a pilot data set consisting of diagnosed MS patients and comparing our results to an extensive 3 T MWI atlas. Evaluating the difference between our data gathered at 7 T and the 3 T atlas might give initial indications on the possibility of generalizing the 3 T atlas across field strengths. Furthermore, it might become a component in the evidence to support or contradict that our method is useful.

II. Data

A. In vivo data acquisition

MR-scans from 11 patients diagnosed with severe MS using TE 8 ms and isotropic voxels, in addition to four scans from healthy volunteers with both TE 8 ms and 10 ms, and isotropic and anisotropic voxels were collected. Except the varying echo time and voxel size the sequence was the same as the one in the Wiggermann et al. study [8].

B. 3 T atlas

By gathering MWF-images from 100 individuals, Dvorak et al. have created an ”optimized anatomical brain template“ and an MWF atlas containing mean values and standard deviation in each voxel [16]. By spatially normalizing new data with the template, any MRI image can be compared against their atlas.

III. Experimental

All data analysis was done using self-developed software running on MatLab 2022a. FSLeyes from FSL 6.0.2 was used to view data and create regions of interest (ROI). Pre-analysis, HD-BET was used to extract the brain from the image [17]. Another software, called DECAES, was then used to solve the inverse problem and extract various parameters for the MWF analysis, such as the T_2 distribution.

A. *Exploring the effect of different voxel dimensions and TE on MWF*

The MR-sequence used for gathering data in our study captures the image with $1.65 \times 1.65 \times 1.65$ mm^3 voxels, matching the total volume of the voxel size, $0.98 \times 0.98 \times 5.00$ mm^3, used by Wiggermann et al. [8]. To investigate if the voxel sizes are comparable to the signal they contain, two scans with these voxel dimensions were compared against each other. This comparison consisted of calculating the signal-to-noise ratio (SNR), fit-to-noise ratio (FNR), and fit-to-signal ratio (FNR/SNR) for each MWF-image. The FNR/SNR measure normalizes differences across patients. These values are used to assess the reliability of the short signal component estimation and goodness-of-fit. The T_2 distribution within the MR scans where extracted voxel-wise with DECAES. When extracting the T_2 distribution, DECAES also produces the SNR and FNR for each voxel. These were the values used.

Our sequence uses a TE of 8 ms, which is 2 ms shorter than what is used in the study by Wiggermann et al. [8]. A shorter TE would imply that DECAES will be able to extract the short and long fraction easier from the total T_2 distribution, and thus the FNR from TE 8 ms should be higher than for 10 ms. Previous studies have used SNR and FNR to understand how well the model is fitted to the measured data, note that this is not a true measure of signal-to-noise but how well the model fits the data. In line with previous studies, to examine if TE 8 ms results in a higher FNR compared to 10 ms the SNR, FNR, and FNR/SNR from two scans with identical voxel dimensions but with TE 8 ms and 10 ms were compared as described in the previous paragraph.

Finally, the aggregated effect from using both a lower TE and isotropic voxels was also examined by comparing scans with TE 8 and isotopic voxels to scans with TE 10 ms and anisotropic voxels. Moreover, the distribution curve from three healthy individuals' frontal lobes was generated with TE 8 ms and 10 ms to study the echo time's effect on the T_2 distribution. Thereto, an average MWF in the region was calculated.

Beyond the parameters that are investigated in this section, when executing DECAES, the following parameters were used (as per Wiggermann 2021 [8]). 40 T_2 times, $T_{2,min} = 8$ ms, $T_{2,cut} = 20$ ms, and maximum $T_2 = 2$ s. The regularisation used was χ^2 with $\chi^2/\chi^2_{min} = 1.02$.

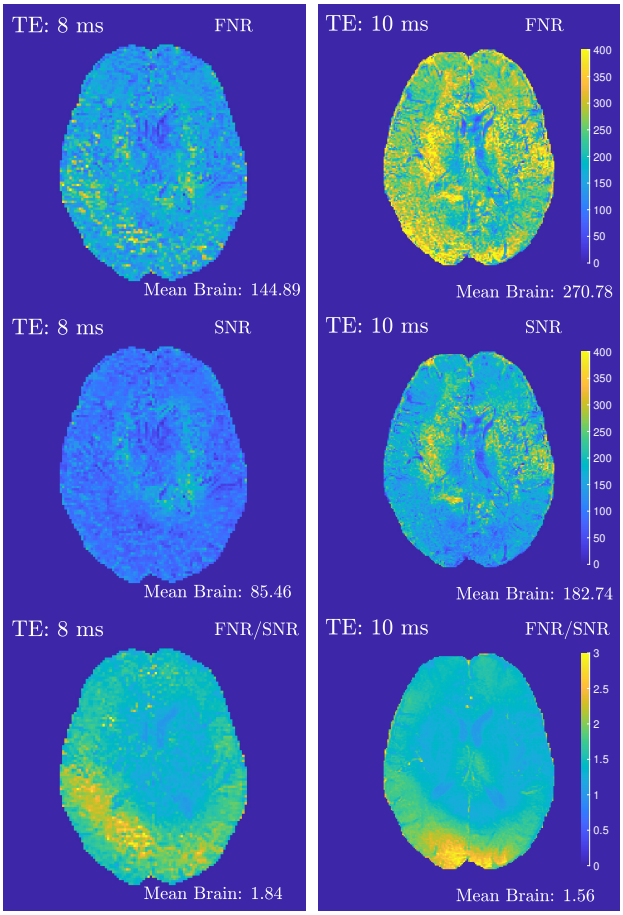

Fig. 2. The total effect of TE 8 ms and isotropic voxels compared to TE 10 ms and anisotropic voxels. The mean value is calculated throughout the whole brain.

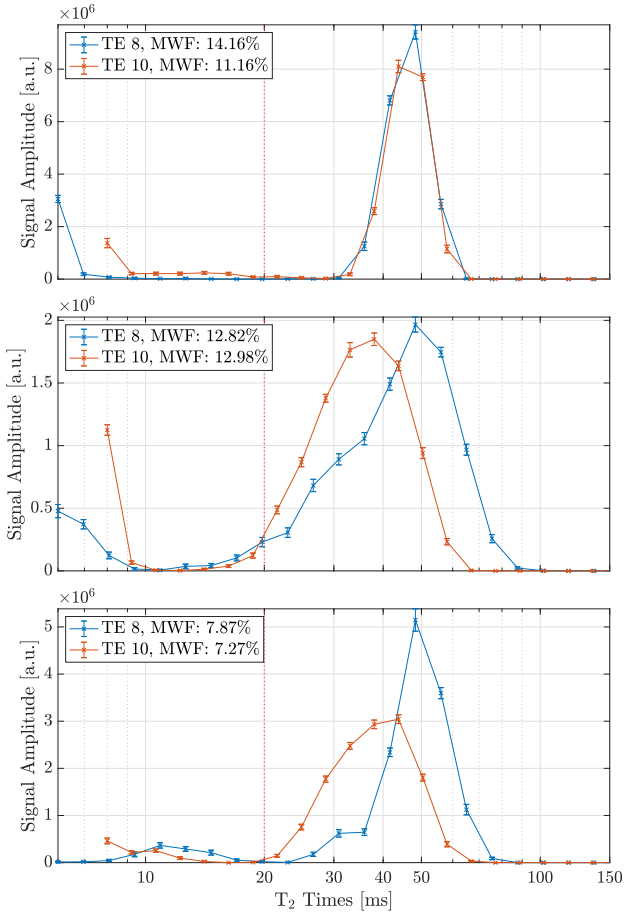

Fig. 3. T_2 distribution from 3 healthy individuals using TE 8 ms with $T_{2,min}$ 6 ms, and 10 ms with $T_{2,min}$ 8 ms. Note that the MWF is calculated for a region within the frontal lobe for each individual.

B. $T_{2,min}$ and $T_{2,cut}$ comparison

When solving the inverse problem and calculating the MWF, the time intervals for the short and long signal components have to be assumed in advance. According to Wiggermann et al., for TE 10 ms at 7 T, the optimal values for $T_{2,min}$ and $T_{2,cut}$ are 8 ms and 20 ms, respectively [8]. To determine these parameters for TE 8 ms, multicomponent analysis with varying $T_{2,min}$ and $T_{2,cut}$ was executed. The parameter values investigated were 6 and 8 ms for $T_{2,min}$, as previous studies have shown that $TE - T_{2,min} \leq 2$, [7], and 20, 25 and 30 ms for $T_{2,cut}$. The resulting MWF-maps were compared to determine the favorable parameter values for scans with TE 8 ms. In the absence of a better method, we identified the optimal $T_{2,min}$ value based on previous studies where $TE - T_{2,min} \leq 2$ [7]. The most favorable value of $T_{2,cut}$ was defined as the value that excludes as much of the intermediate peak (figure 1) and includes as much of the short fraction hump as possible.

C. Lesion analysis with established parameters

As a final trial to validate the established parameters, we assessed the ability to distinguish MS lesions with MWI using these newfound parameters, as such lesions have a lower amount of myelin. One FLAIR image and one MWF-map were obtained from four MS patients. FLAIR was chosen as it is suitable for qualitative lesion detection. Another analysis was conducted by comparing the MWF of a defined lesion to an area of the same size mirrored in the midsaggital plane.

D. MWI atlas comparison

Finally, the MR-scans from healthy individuals were compared to the 3 T MWI atlas [16] to investigate how well existing data at 3 T may be used for MR-scans at 7 T with our sequence. The MR scans from healthy individuals at 8 ms were first spatially normalized to the atlas using ANTs [18]. This step ensured that each region in the image corresponds to the same in the atlas. Subsequently, the number of standard deviations that our MWF data deviated from the atlas was calculated for each voxel, the Z-score. A mean Z-score was determined for white matter and gray matter, respectively. A Z-score map was generated and viewed in FSLeyes together with an anatomical image (T_1 template) to assess if the data contains any structural information [19].

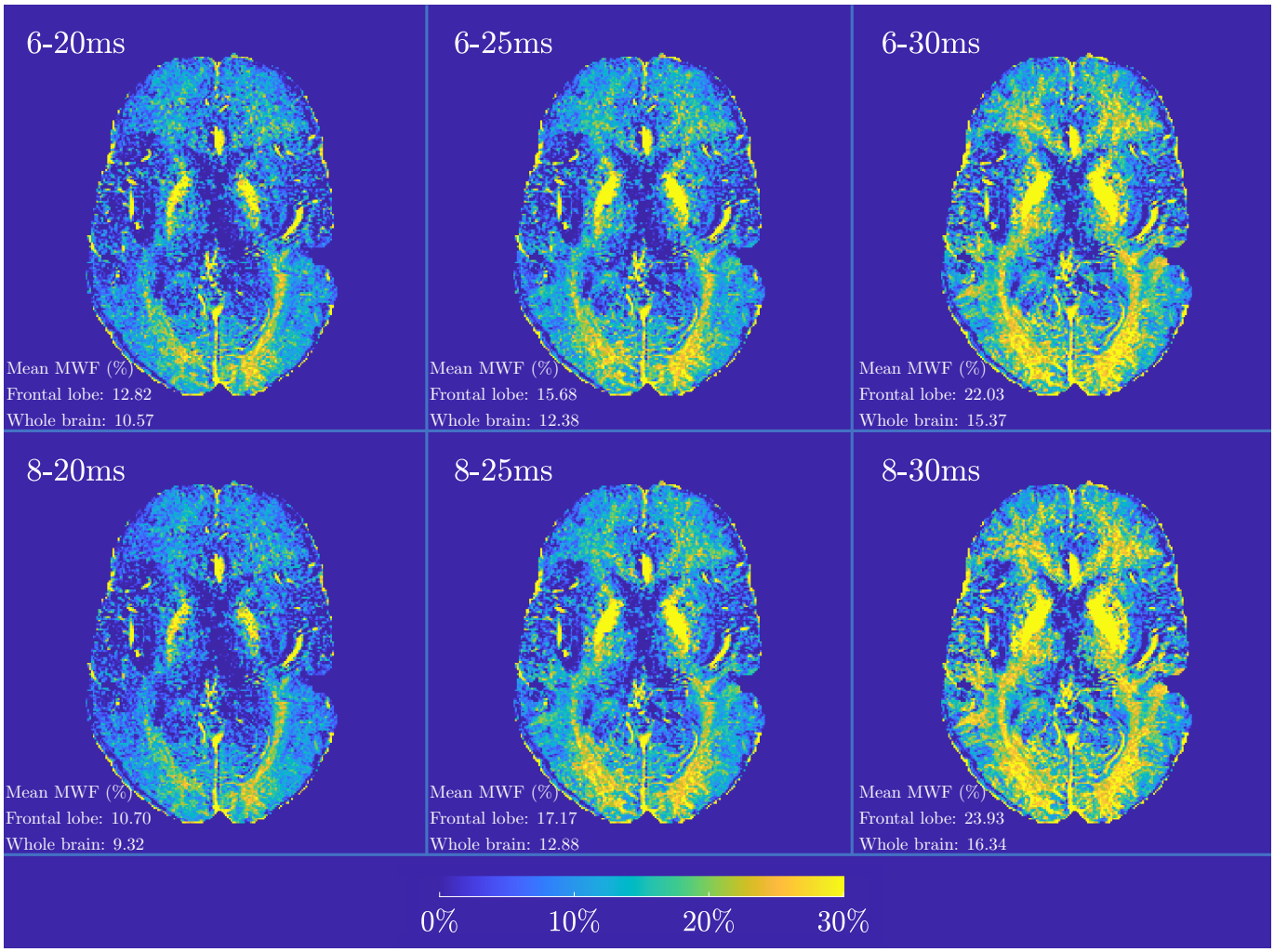

Fig. 4. Myelin water fraction map of one healthy subject with different $T_{2,min}$ and $T_{2,cut}$

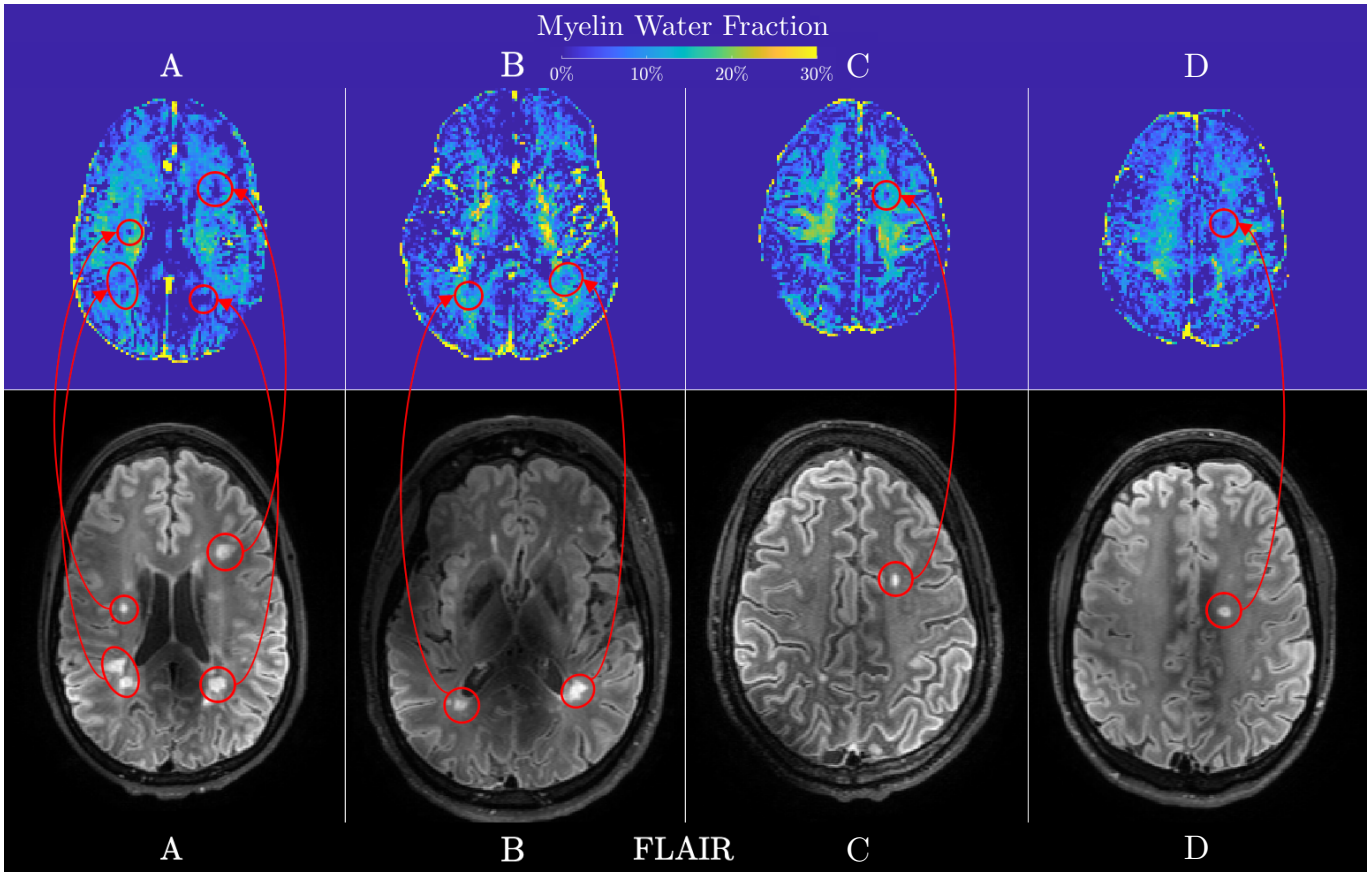

Fig. 5. Each column A-D contains a FLAIR image and a corresponding MWF-map for four different patients. The white spots in the FLAIR image are potential lesions that show as dark spots on the MWF-map.

IV. Result

A. The effects on MWF result from different voxel dimensions and TE

When using the isotropic compared to the anisotropic voxels, there seems to be a difference in SNR and FNR between isotropic and anisotropic voxels. However, the FNR/SNR ratios for both voxel dimensions are similar, with a mean value of 1.54 compared to 1.40. A similar result is found when studying the different TE times, where the mean FNR/SNR was 1.39 for TE 8 ms and 1.42 for TE 10 ms. Figure 2 shows the total effect of using TE 8 ms and cubical voxels compared to TE 10 ms and rectangular voxels. The mean FNR/SNR was 1.84 and 1.56, respectively.

The T_2 distribution using TE at 8 ms compared to 10 ms in the frontal lobe is shown in figure 3. A lower TE time should capture more of the fast decaying T_2 component, such as myelin water. The consequence of this would be an increased average myelin estimate within each voxel. However, the MWF in one of the distributions is lower when using TE 8 ms than 10 ms.

B. $T_{2,min}$, $T_{2,cut}$ and its relationship with the myelin water fraction

A comparison of the different $T_{2,min}$ and $T_{2,cut}$ times is shown in figure 4. As expected, there is a positive relationship between $T_{2,cut}$ and the mean MWF. This correlation is possibly due to more of the intermediate peak being incorrectly included in the MWF. Another trend that is seen is that as $T_{2,min}$ decreases, the rate at which the mean MWF increases–possibly due to an increase in $T_{2,cut}$– increases. In other words, the effect on mean MWF due to spillover from the long fraction is more pronounced at higher $T_{2,min}$.

C. Using MWF to identify lesions

Implementing MWI for patients diagnosed with MS clarifies that a decrease in MWF can be found in lesions. In figure 5, the visible lesions in the FLAIR image can also be found in the MWF-map where the MWF is decreased. Furthermore, table I shows an apparent decrease of MWF within lesions compared to the mirrored NAMW region.

TABLE I
MWF within a lesion compared to MWF in the region mirrored in the midsaggital plane containing normal appearing white matter

MWF in lesion [%]	MWF in mirrored NAWM [%]
4.565	10.186
7.723	12.619
3.985	13.910

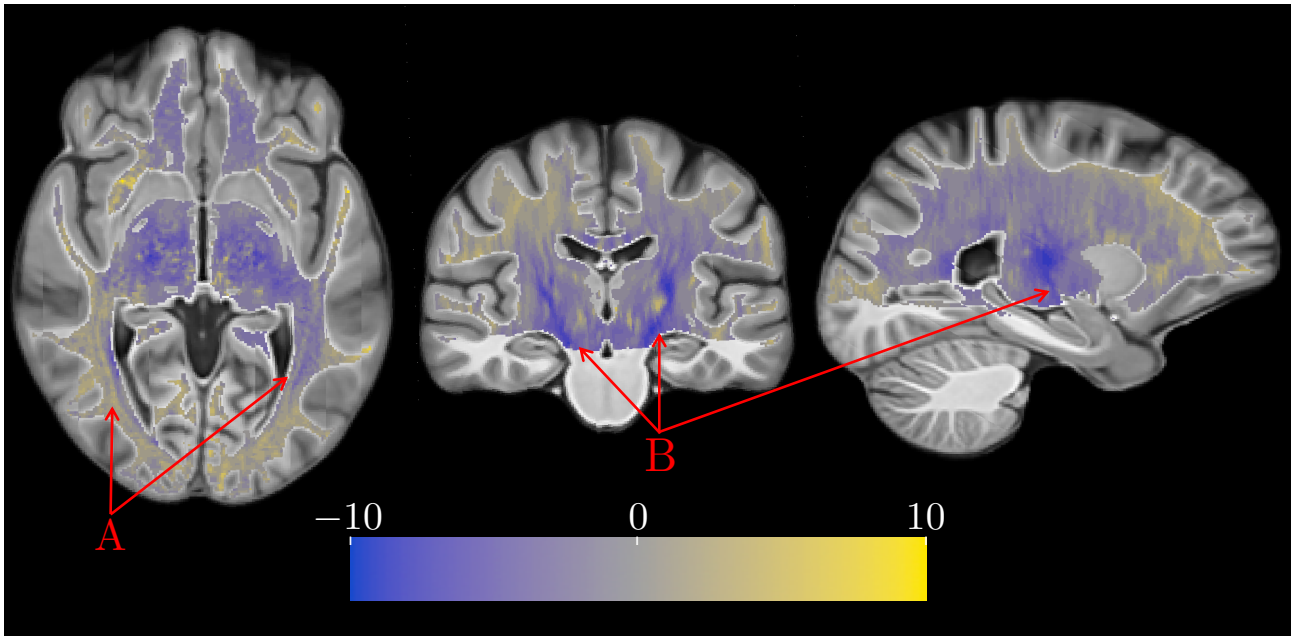

Fig. 6. The T1 atlas template together with the 7 T standard deviations within white matter as an overlay. A: Shows the deviations within the optic radiation. B: Shows the deviations within the corticospinal tract.

D. 7 T scans compared to 3 T atlas

The MWF values of the white matter determined from MR-scans obtained at 7 T and compared to the 3 T atlas have a difference in myelin of 0.009 ± 1.968. A different result can be found when looking at gray matter, where 7 T had a significantly greater difference in myelin of 1.664 ± 3.146. We observe some clear anatomical patterns within the optic radiation and corticospinal tract when looking at the images. A pattern of increase and decrease seems to exist, as shown in figure 6. The optic radiation has a higher average MWF than the 3 T atlas (A), and the corticospinal tract is, on average lower (B).

V. Discussion

A shorter TE encompasses more of the fast decaying signal, i.e., from myelin water. This would imply a higher average MWF estimation within all regions containing myelin compared to scans with longer TE. In figure 3, where the TE 8 ms and 10 ms are compared, the expected results do not occur in all three subjects. The MWF in the frontal lobes of the three healthy subjects varies in no specific way. Since the same ROI was used to encompass a relatively uniform region for both sequences for each individual, this result is surprising. If this is not due to a measuring artifact or some other source of error, it indicates that a 10 ms TE might be enough to determine the MWF accurately.

Another aspect that is important to have in mind when comparing estimations of MWF from different individuals is that the actual amount of myelin varies. Age, education, and sex of an individual are a few factors that impact the amount of myelin in the brain [20]. Therefore, a small comparison between individuals, such as ours, holds less significant value. A future study may clarify the effect of different TEs on the decay curve. However, given our findings, it is shown that our sequence can accomplish similar results as those presented in Wiggermann's article [8].

The average MWF should increase when a lower TE time is used since more information from the fast decaying signals can be differentiated. Consequently, the SNR and FNR should also increase when using the lower TE time. However, as shown in figure 2 there seems to be a decrease in both SNR and FNR. This is because the SNR and FNR are both scaled by the arbitrary signal level of the acquired data, which is revealed by the similar FNR/SNR values between the two echo times.

When analyzing different short and long fractions by changing the $T_{2,min}$ and $T_{2,cut}$, there is a clear trend that a longer short fraction results in a higher average MWF. The trend arises because the water in the cytoplasmic and extracellular space has a longer T_2 decay, as shown in figure 1, and by using a long $T_{2,cut}$, there is overspill from this region in the myelin estimation. The use of $T_{2,min}$ at 6ms ensures that the additional information from TE 8ms can be captured and defined. Previous studies have shown that $TE - T_{2,min} \leq 2$, [7] and our findings concur.

As shown in figure 5, MWI can be used to identify MS lesions when using scans from 7 T. Each lesion shows a decrease of estimated myelin in the MWF-map. Thus the lesions can be associated with a decrease in myelin. Interestingly, some dark spots in the MWF-map do not correspond to a lesion as there are no white spots in that place in the FLAIR image. Consequently, the MWF-map can not by itself be used as a diagnostic tool. Another result that needs to be further discussed is the amount of darkening in the MWF-map of different lesions. Some lesions have almost no MWF, whereas others have only a slight decrease in MWF. This could help identify and separate new lesions from old ones, furthering the ability to follow the progression of the disease. This is well

established at 3 T [13]. However, with increased resolution, more detailed information can be extracted.

A. Is the 3 T atlas suitable for 7 T scans?

While the comparison between 7 T data and 3 T atlas shows that the average deviation is close to 0 within the white matter, we observe apparent spatial variations when studying specific structures such as the optic radiation, 6-A, and corticospinal tract, 6-B. There seem to be some trends of deviation. This indicates that the existing atlas can not be used for 7 T scans.

B. Future work

A continuation of this work would be to investigate further the structural information uncovered by our 3 T atlas-comparison seen in figure 6 by comparing the 3 T atlas with a broader collection of 7 T data.

C. Ethics and sustainability

MRI at 7 T is a safe medical imaging technique for depicting anatomy, as it does not expose patients to high-energy ionizing radiation. However, the patient may experience some muscle-twitching. Safety at 7 T and 3 T are considered similar [21].

It is important to note that MRI data is considered sensitive personal data as the head and face shape may be visible in the data. This makes anonymizing MRI data a tedious process, where removing the patient ID is only one of the steps.

The time it takes to capture images with MRI is based on the sequence used. Using a sequence with lower TE, such as ours, allows the total scan time to be a fraction shorter than a higher TE. This would imply less energy being used for the MRI, less discomfort for the patient, and enabling more patients to be examined.

While MWI might present an opportunity for automatic diagnosis, this would require the drafting of new guidelines as no diagnosis can be set solely by computer calculations.

VI. Conclusion

We have demonstrated that MWI on 7 T scans with isotropic voxels and an 8 ms TE can be used to identify lesions associated with MS. However, there is not enough evidence to neither validate nor reject that an 8 ms TE is superior to a 10 ms when it comes to characterizing the myelin water fraction. More research into this topic is warranted.

VII. Acknowledgments

We, Elliot Berthold and Petter Clemensson, study Biomedical engineering at LTH, Lund. This paper corresponds to our bachelor's thesis, and it was carried out during the spring term 2022.

We are grateful for the data provided by our clinical supervisor Gunther Helms, and everything he has done to help us along the way.

Finally, we would like to give a special thanks to our outstanding supervisor Emil Ljungberg for the continuous guidance and extensive feedback along the way.

References

[1] C. Myburgh, T. B. Larsen, and P. Kjaer, "'when the picture does not really tell the story'–a qualitative exploration of the mri report of findings as a means for generating shared diagnostic meaning during the management of patients suffering from persistent spinal pain," *Patient Education and Counseling*, vol. 105, no. 1, pp. 221–227, 2022.

[2] W. J. Brownlee, T. A. Hardy, F. Fazekas, and D. H. Miller, "Diagnosis of multiple sclerosis: progress and challenges," *The Lancet*, vol. 389, no. 10076, pp. 1336–1346, 2017.

[3] E. M. Edwards, W. Wu, and N. E. Fritz, "Using myelin water imaging to link underlying pathology to clinical function in multiple sclerosis: A scoping review," *Multiple Sclerosis and Related Disorders*, vol. 59, p. 103646, 2022.

[4] A. Mackay, K. Whittall, J. Adler, D. Li, D. Paty, and D. Graeb, "In vivo visualization of myelin water in brain by magnetic resonance," *Magnetic Resonance in Medicine*, vol. 31, no. 6, pp. 673–677, jun 1994.

[5] M. Bouhrara, A. C. Rejimon, L. E. Cortina, N. Khattar, C. M. Bergeron, L. Ferrucci, S. M. Resnick, and R. G. Spencer, "Adult brain aging investigated using bmc-mcdespot–based myelin water fraction imaging," *Neurobiology of aging*, vol. 85, pp. 131–139, 2020.

[6] E. Alonso-Ortiz, I. R. Levesque, and G. B. Pike, "Mri-based myelin water imaging: a technical review," *Magnetic resonance in medicine*, vol. 73, no. 1, pp. 70–81, 2015.

[7] V. Wiggermann, I. Vavasour, S. Kolind, A. MacKay, G. Helms, and A. Rauscher, "Non-negative least squares computation for in vivo myelin mapping using simulated multi-echo spin-echo t_2 decay data," *NMR in Biomedicine*, vol. 33, no. 12, mar 2020.

[8] V. Wiggermann, A. L. MacKay, A. Rauscher, and G. Helms, "In vivo investigation of the multi-exponential T_2 decay in human white matter at 7 T: Implications for myelin water imaging at UHF," *NMR in Biomedicine*, vol. 34, no. 2, oct 2020.

[9] O. Kraff, A. Fischer, A. M. Nagel, C. Mönninghoff, and M. E. Ladd, "Mri at 7 tesla and above: demonstrated and potential capabilities," *Journal of Magnetic Resonance Imaging*, vol. 41, no. 1, pp. 13–33, 2015.

[10] E. Ljungberg, I. Vavasour, R. Tam, Y. Yoo, A. Rauscher, D. K. Li, A. Traboulsee, A. MacKay, and S. Kolind, "Rapid myelin water imaging in human cervical spinal cord," *Magnetic Resonance in Medicine*, vol. 78, no. 4, pp. 1482–1487, nov 2016.

[11] R. G. Spencer and C. Bi, "A tutorial introduction to inverse problems in magnetic resonance," *NMR in Biomedicine*, vol. 33, no. 12, aug 2020.

[12] K. P. Whittall and A. L. MacKay, "Quantitative interpretation of NMR relaxation data," *Journal of Magnetic Resonance (1969)*, vol. 84, no. 1, pp. 134–152, aug 1989.

[13] A. L. MacKay and C. Laule, "Magnetic resonance of myelin water: An in vivo marker for myelin," *Brain Plasticity*, vol. 2, no. 1, pp. 71–91, dec 2016.

[14] Roadnottaken, "Myelinated neuron," 2007. [Online]. Available: https://commons.wikimedia.org/w/index.php?curid=3845936

[15] J. Wonderlick, D. A. Ziegler, P. Hosseini-Varnamkhasti, J. Locascio, A. Bakkour, A. Van Der Kouwe, C. Triantafyllou, S. Corkin, and B. C. Dickerson, "Reliability of mri-derived cortical and subcortical morphometric measures: effects of pulse sequence, voxel geometry, and parallel imaging," *Neuroimage*, vol. 44, no. 4, pp. 1324–1333, 2009.

[16] A. V. Dvorak, T. Swift-LaPointe, I. M. Vavasour, L. E. Lee, S. Abel, B. Russell-Schulz, C. Graf, A. Wurl, H. Liu, C. Laule, D. K. B. Li, A. Traboulsee, R. Tam, L. A. Boyd, A. L. MacKay, and S. H. Kolind, "An atlas for human brain myelin content throughout the adult life span," *Scientific Reports*, vol. 11, no. 1, jan 2021.

[17] F. Isensee, M. Schell, I. Pflueger, G. Brugnara, D. Bonekamp, U. Neuberger, A. Wick, H.-P. Schlemmer, S. Heiland, W. Wick, M. Bendszus, K. H. Maier-Hein, and P. Kickingereder, "Automated brain extraction of multisequence mri using artificial neural networks," *Human Brain Mapping*, vol. 40, no. 17, pp. 4952–4964, 2019. [Online]. Available: https://onlinelibrary.wiley.com/doi/abs/10.1002/hbm.24750

[18] B. B. Avants, N. Tustison, G. Song *et al.*, "Advanced normalization tools (ants)," *Insight j*, vol. 2, no. 365, pp. 1–35, 2009.

[19] P. McCarthy, "Fsleyes," 2022.

[20] T. D. Faizy, C. Thaler, D. Kumar, J. Sedlacik, G. Broocks, M. Grosser, J.-P. Stellmann, C. Heesen, J. Fiehler, and S. Siemonsen, "Heterogeneity of multiple sclerosis lesions in multislice myelin water imaging," *PloS one*, vol. 11, no. 3, p. e0151496, 2016.

[21] M. J. van Osch and A. G. Webb, "Safety of ultra-high field mri: what are the specific risks?" *Current Radiology Reports*, vol. 2, no. 8, pp. 1–8, 2014.